

Seismic vulnerability of RC buildings considering SSI and aging effects



S.D. Fotopoulou, S.T. Karapetrou & K.D. Pitilakis

Aristotle University of Thessaloniki, Greece

SUMMARY: (10 pt)

The present study aims at the assessment of seismic vulnerability of RC buildings taking into account the soil – structure –interaction (SSI) and the aging effects due to corrosion of the RC structural members. Two-dimensional non-linear dynamic analyses were performed to assess the expected performance of initial ($t=0$ years) and 50 years old RC frame structures. The time-dependent probabilistic fragility functions are derived for adequately predefined damage states at different time periods in terms of peak ground acceleration at the base of the studied structure typologies. As it was expected, the fragility of the structures increases over time due to corrosion. Moreover, the consideration of soil deformability and SSI effects is found to yield to a significant increase on the seismic vulnerability. Hence the combination of these two effects may modify detrimentally the vulnerability of RC structures compared to the usually assumed case of fixed base structure with no aging affects.

Keywords: seismic vulnerability, RC buildings, time-dependent fragility curves, aging, SSI effects

1. INTRODUCTION

The seismic vulnerability of structures is commonly expressed through probabilistic fragility functions representing the conditional probability of reaching or exceeding a predefined damage state given the measure of earthquake shaking. It's evaluation is essential for effective emergency planning, risk management and mitigation of damage and losses prior and after an earthquake. Traditionally, in seismic vulnerability assessment studies it has been implicitly assumed that the maintenance of the structure is conducted in an optimum manner. In other words, the impact of various environmental deterioration mechanisms (such as e.g. corrosion, erosion, fatigue or even cumulative damages from past seismic events), on the seismic fragility estimates have not been yet accounted for. These phenomena are dynamic in nature and as such a time-dependent fragility analysis of the structure is required to account for their changing patterns over time and their likely evolving potential for structural damage. One of the most important environmental degradation mechanisms of RC buildings is corrosion of the steel reinforcement. Corrosion is a complex process that may affect a RC structure in a variety of ways, including, among others, cover spalling, loss of steel-concrete bond strength and loss of reinforcement cross sectional area. Thus, it may affect both the safety and serviceability of RC structures in relation to their initial as-built state under the action of seismic (or even static) loading. It has been generally acknowledged that corrosion phenomena are subject to severe uncertainties thus necessitating the use of probabilistic models (e.g. Duracrete 2000). Very recently some researchers (e.g. Ghosh and Padgett, 2010; Choe et al, 2010; Yalciner et al 2012) have introduced different probabilistic models into the seismic vulnerability assessment framework to assess the time-variant seismic fragility of corroded bridges and RC frame structures.

In parallel, other important effects that can significantly contribute to the building's seismic fragility are the soil conditions affecting the foundation compliance and the soil-structure interaction. Although there are some studies that take into account the local site effects by providing fragility curves for buildings for different soil conditions (e.g. NIBS, 2004), the effect of soil-structure interaction (SSI) to

the expected structure's performance has not received much attention. This may be due to the fact that the incorporation of SSI phenomena in the analysis is generally believed to reduce the seismic demand and consequently the corresponding structural damage of non-linear systems. Thus, neglecting their effects in fragility modeling has been generally assumed to be on the safe side. However, it has been shown that SSI effects may be either beneficial or unfavorable to the structure's seismic fragility depending on the dynamic properties of the soil and the building as well as the characteristics (frequency content, amplitude, significant duration) of the input motion (Saez et al, 2011).

The scope of this study is to assess the seismic vulnerability of RC buildings taking into account the SSI and the aging of the RC structural members proposing time-dependent fragility functions. Figure 1 presents a schematic flowchart of the proposed framework adopted to develop time-dependent fragility curves for RC frame buildings. Soil structure interaction is considered through an uncoupled approach. The appropriate motion at the foundation level of the structure is estimated through a 1D equivalent linear analysis for given soil profiles (corresponding to shear wave velocities $V_{so,ave}=200$ and 300m/s), while the soil structure interaction has been modeled using appropriate springs and dashpots, that simulate rocking and sway corresponding to the computed ground shear strain levels. The consideration of aging is achieved by including probabilistic models of chloride induced corrosion deterioration of the RC elements within the vulnerability modeling framework. Two-dimensional non-linear dynamic time history analyses were performed for all the RC building typologies considered herein. Different real accelerograms recorded in outcrop conditions scaled at three different levels of peak ground acceleration PGA ($0.1g$, $0.3g$ and $0.5g$) are used as input motion. Fragility curves derived for the initial ($t=0$ years) and the corroded buildings ($t=50$ years) are compared to gain insight into the effect of reinforcement corrosion on the structure's performance. Moreover, different time-dependent curves are constructed to account for the effects of SSI and soil conditions (rock, $V_{so}=300\text{m/s}$, $V_{so}=200$ m/sec) highlighting the importance of their incorporation in the fragility analysis.

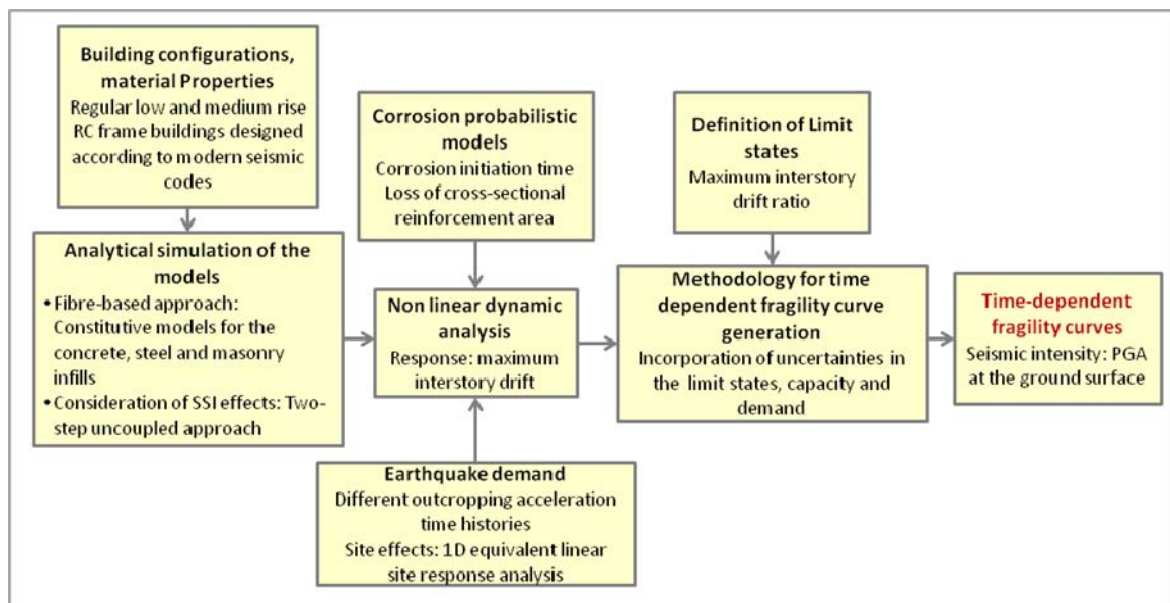


Figure 1.1 Methodological framework adopted

2. APPLICATION

2.1. Description of the numerical models

The studied reference structures are two moment resisting frames (MRFs) that vary on the geometrical, structural and stiffness characteristics (Fig. 2.1). The first one (adopted by Gelagoti 2010) is a two storey - one bay frame model that is considered representative of low – rise buildings, designed by the Greek seismic code (EAK, 2000). The second is a four storey frame model with

three bays that can be categorized as a mid – rise building, designed according to the current seismic code of Portugal (adopted by Abo El Ezz, 2008). The analyses of the buildings are conducted using the finite element code SeismoStruct (Seismosoft, 2011), which is capable of calculating the large displacement behavior of space frames under static or dynamic loading, taking into account both geometric nonlinearities and material inelasticity. The spread of material inelasticity along the member length and across the section area is represented through the employment of a fibre-based modeling approach, implicit in the formulation of SeismoStruct's inelastic beam-column frame elements. Thus, the sectional stress-strain state of beam-column elements is obtained through the integration of the nonlinear uniaxial material response of the individual fibres in which the section is subdivided. For the present analysis, the frame sections are divided into 300 fibres. Distributed inelasticity frame elements are implemented assuming force-based (FB) formulations and considering 4 controlling integration sections along the element. A uniaxial nonlinear constant confinement model is used for the concrete material, assuming a constant confining pressure throughout the entire stress-strain range (Mander et al.,1988). For the reinforcement, a uniaxial bilinear stress-strain model with kinematic strain hardening is utilized. The mass of the building is assumed to be uniformly distributed along beam elements. Some basic characteristics of the reference structures are presented in Table 2.1.

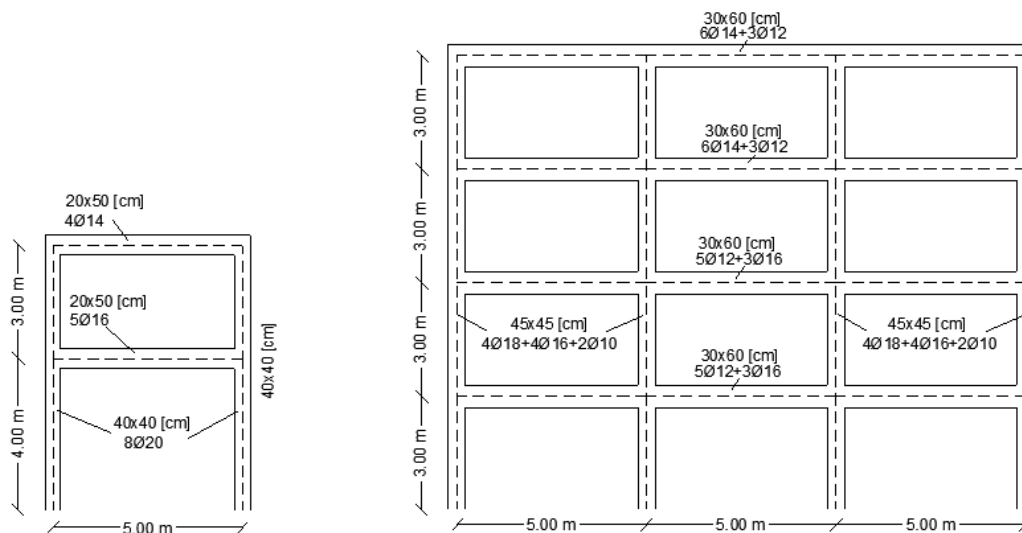


Figure 2.1 Reference MRF models used for time – dependent vulnerability assessment

Table 2.1 Characteristics of the studied buildings

RC building		Sections [cm]	Mass [t/m]	Initial fundamental period T [sec]	f_c [MPa]	f_y [MPa]
Low-rise	Column	40x40	0.41	0.3936	20	500
	Beam 1st - 2nd floor	20x50	3.15			
Mid-rise	Column	45x45	0.51	0.5018	28	460
	Beam 1st - 2nd - 3rd floor	30x60	4.77			
	Beam 4th floor	30x60	3.41			

To consider the reference fixed base condition the structures are assumed to be founded on rock. Then four structural models are analyzed considering SSI effects for two representative soil profiles. Appropriate link elements (rotational and translational springs and dashpots) are used to simulate the foundation rigidity and damping with respect to the underlain soil and the attained ground shear strains as described in the following subsection.

2.2. Consideration of SSI effects

The influence of SSI in the dynamic response of the structure is taken into account in an uncoupled two-step approach. First, the bedrock time-histories are propagated through a one - dimensional

equivalent linear analysis for the considered soil profiles, using Cyberquake (BRGM Software 1998). It is noticed that due to the consideration of an elastic halfspace ($V_s=1000$ m/sec) it was possible to directly apply the outcropping rock motion at the base of the soil model (Kwok et al. 2007). Then, the obtained free field surface motion is imposed at the base of the buildings to estimate the expected seismic performance. The coupling of the two sub models (soil and structure) is achieved by calculating impedance functions introduced into the base of the structural models via equivalent linear springs and dashpots. To simulate the soil-foundation conditions, two soil deposits are considered (Fig. 2.2). The average low strain shear wave velocities $V_{so,ave}$ of the soil profiles are taken equal to 300m/sec and 200m/sec respectively. The elastic bedrock ($V_s=1000$ m/sec) is assumed to lie at 30m. The nonlinear soil behavior is modeled using the shear modulus reduction and damping curves proposed by Darandeli (2001), which account for the variation of soil plasticity, OCR and overburden pressure with shear strain amplitude. The analysis yields the free field acceleration time histories at the ground surface that are finally inserted into the structural models. In parallel, the amplitude of the effective shear strain of the surface layer ($\gamma_{eff}=0.65 \cdot \gamma_{max}$) is used for the calculation of the new compatible values of shear modulus and material damping ratio. Based on the new dynamic soil properties, the stiffness and radiation damping of equivalent springs (K_i) and dashpots (C_i) respectively are estimated through the expressions proposed by Mylonakis et al. (2006) referring to equal size footings on elastic half – space. The footing dimensions are selected to satisfy the prescriptions of the modern seismic norms as 1.7m x1.7m and 2m x 2m for the low and medium rise structures respectively.

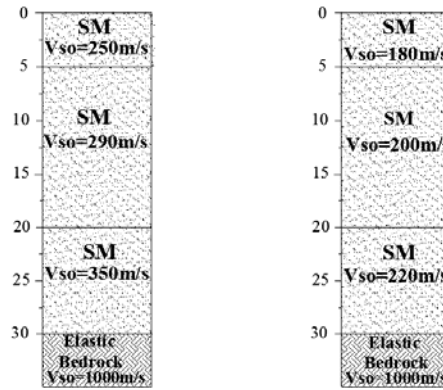


Figure 2.1 Soil profiles used for the 1D equivalent linear site response analyses

2.3. Corrosion modeling

Several models have been proposed to quantify and account for corrosion in the design, construction, fragility analysis and maintenance of RC structures. A summary of these models can be found e.g. in DuraCrete (1998). In the present study the corrosion of reinforcing bars due to the ingress of chlorides is considered, as it is reportedly one of the most serious and widespread deterioration mechanisms of concrete structures. The probabilistic model proposed by FIB- CEB Task Group 5.6 (2006) for modeling corrosion initiation due to chloride ingress is adopted. According to this, the time till corrosion initiation can be determined as:

$$T_{ini} = \left(\frac{\alpha^2}{4 \cdot k_e \cdot k_t \cdot D_{RCM,0} \cdot (t_0)^n} \cdot \left(\text{erf}^{-1} \left(1 - \frac{C_{crit}}{C_s} \right) \right)^{-2} \right)^{\left(\frac{1}{1-n} \right)} \quad (2.1)$$

where T_{ini} =corrosion initiation time (years), α =cover Depth (mm) C_{crit} =critical chloride content (wt % cement); C_s = the equilibrium chloride concentration at the concrete surface (wt % cement); t_0 =reference point of time (years); $D_{RCM,0}$ =Chloride migration Coefficient (m^2/s); k_e =environmental function; k_t =regression parameter; erf =Gaussian error function and n =aging exponent.

Once the protective passive film around the reinforcement dissolves due to continued chloride ingress, corrosion initiates and the time dependent loss of reinforcement cross-sectional area can be expressed as (e.g. Ghosh and Padgett, 2010):

$$A(t) = \begin{cases} n \cdot D_i^2 \cdot \frac{\pi}{4} & \text{for } t \leq T_{ini} \\ \max \left[n \cdot (D \cdot (t))^2 \cdot \frac{\pi}{4}, 0 \right] & \text{for } t \geq T_{ini} \end{cases} \quad (2.2)$$

where n =number of reinforcement bars; D_i =initial diameter of steel reinforcement; t =elapsed time in years and $D(t)$ =reinforcement diameter at the end of $(t - T_{ini})$ years, which can be defined as:

$$D(t) = D_i - i_{corr} \cdot \kappa \cdot (t - T_{ini}) \quad (2.3)$$

where i_{corr} =rate of corrosion (mA/cm^2); κ =corrosion penetration ($\mu\text{m}/\text{year}$) ($\kappa = 11$, $6\mu\text{m}/\text{year}$ uniform corrosion penetration for generalized corrosion).

The statistical quantification of the model parameters describing the chloride induced corrosion initiation and propagation into the reinforced concrete elements adopted for the present study is given in Table 2.2 based on FIB- CEB Task Group 5.6 (2006) prescriptions and the available literature (e.g. Choe et al., 2009, 2010; Stewart, 2004; Ghosh and Padgett, 2010). A relatively aggressive atmospheric exposure environment (e.g. $k_e=0.67$, Choe et al., 2009) is assumed for an adverse chloride induced deterioration scenario ($w/c=0.6$, High corrosion Level). The distribution for the corrosion initiation time is assessed through crude Monte Carlo simulation. A lognormal distribution with mean 2.96 years and standard deviation of 2.16 years is found to be a good fit to the simulated data for the corrosion initiation time.

Table 2.2 Statistical characteristics of parameters affecting the chloride induced corrosion deterioration of RC elements adopted in the present study

Parameter	Mean	COV	Distribution
Cover Depth (mm) α	25	0.20	Lognormal
Environmental transfer variable k_e	0.67	0.10	Normal
Chloride migration Coefficient ($D_{RCM,0}$) (m^2/s)	2.5E-11	0.10	Normal
Aging exponent n	0.3	cov=0.05, a=0.0, b=1.0	Beta
Critical Chloride Concentration (C_{cr}) wt % cement	0.6	cov=0.05, a= 0.2, b=2.0	Beta
Surface Chloride Concentration (C_s) wt % cement	1.539	0.10	Normal
Rate of Corrosion (i_{corr}) mA/cm^2	10	0.20	Normal

Table 2.3 Reinforcement area in different points in time ($t= 0$ and 50 years) for the low and mid-rise RC buildings

RC Building	Element	Reinforcement ($t=0$ years)	Reinforcement area		Loss of Reinforcement area at $t=50$ years
			A_o ($t=0$ years) (mm^2)	$A(t=50\text{years})$ (mm^2)	$A(t)/A_o$
Low-rise	Column	8 Φ 20	2513.20	1340.00	0.53
	1st floor beam	5 Φ 16	1005.31	447.65	0.45
	2nd floor beam	4 Φ 14	615.75	238.72	0.39
Mid-rise	Column	4 Φ 18	1017.88	502.78	0.49
		4 Φ 16	804.25	358.14	0.45
	1st and 2nd floor beams	2 Φ 10	157.08	37.99	0.24
		5 Φ 12	565.49	180.59	0.32
		3 Φ 16	603.19	268.62	0.45
		3rd and 4th floor beams	6 Φ 10	471.24	113.86
	3 Φ 12	339.29	108.22	0.32	

The distribution of the loss of area of steel due to corrosion of the RC elements for the considered corrosion scenario ($t=50$ years) is calculated as a function of the corrosion rate and the corrosion initiation time variables as well as the reinforcement of the initial as-built structure. Table 2.3 presents the reinforcement area for the different structural members of the low and mid-rise buildings for the initial non-degraded state and the predicted median values of the reinforcement area (considering a lognormal fit) for the corroded structures. The corresponding anticipated loss within the elapsed time ($t-T_{ini}$) is also shown indicating losses of the cross-sectional area that vary from 24% to 53%. It is assumed that the loss of steel area is uniformly distributed along the reinforced concrete members whereas the degradation of steel material properties is not taken into account.

2.4. Non-linear dynamic analysis

Two-dimensional non-linear dynamic time history analyses are conducted in Seismostruct to predict the inelastic response of the considered RC buildings for the two time scenarios ($t=0$ and 50 years). For the 50 years scenario, the expected median (reduced) values of the longitudinal reinforcing bar cross-sectional area as estimated in the previous section are inserted in the structural dynamic model. Analyses are performed for eight real ground motion accelerograms scaled at different levels of PGA (0.1, 0.3 and 0.5g) and recorded at sites classified as rock (Soil class A) according to EC8 (Table 2.4). In this way, the characteristics of the earthquake ground motion (amplitude, frequency content and duration) in relation to the dynamic properties of the soil and the structures as well as the inherent variability associated to the earthquake demand are explicitly considered on the structures' dynamic response. Note that when the SSI effects are considered, the aforementioned accelerograms are first propagated through 1D soil profiles to obtain the appropriate free field base motion for the structure.

Table 2.4 Selected outcropping records used for the dynamic analyses

Earthquake	Record station	Mw	R (km)	PGA (g)
Valnerina, Italy 1979	Cascia	5.9	5.0	0.15
Friuli, Italy 1976	San Rocco	5.9	15.0	0.11
Parnitha, Athens 1999	Kypseli	6.0	10.0	0.12
Montenegro 1979	Hercegnovi Novi	6.9	60.0	0.26
Northridge, California 1994	Pacoima Dam	6.7	19.3	0.42
Palm Springs, California 1986	Whitewater Trout Farm	6.2	7.3	0.52
Campano Lucano, Italy 1980	Sturno	7.2	32.0	0.32
Umbria, Italy 1998	Cubbio-Piene	4.8	10.0	0.24

The hysteretic damping, which is responsible for the dissipation of the majority of energy introduced by the earthquake action, has already been implicitly included in the analysis through the 1D equivalent linear site response analysis and the employment of the nonlinear fibre-based model formulation of the inelastic frame elements. Additionally, a 3% of tangent stiffness – proportional damping (Priestley and Grant, 2005) is also assigned. Various parameters were analyzed such as the peak ground acceleration PGA, peak ground displacement PGD, spectral acceleration $S_a(T)$ at the base and at the top of the structures and the transfer functions with regard to input's frequency content. However, the final output of the dynamic analysis that is then used to estimate a damage index for assessing the seismic fragility of the buildings, is the maximum interstory drift ratio ($ISD_{max}\%$).

3. DEVELOPMENT OF TIME-DEPENDENT FRAGILITY CURVES

3.1. Definition of damage states

The definition of damage states constitutes an important step in the construction of the fragility curves. The definition and selection of realistic damage states are of paramount importance since these values have a direct effect on the evaluation of the fragility curve parameters. The use in this study, of the maximum interstory drift ratio ($ISD_{max}\%$) to determine the expected global seismic performance of the structures, while it is generally intuitive, is still a comprehensive and easily calibrated indicator that has been widely used in previous studies. Four damage states (slight, moderate, extensive, complete) are defined based on the drift limits proposed by Ghobarah (2004). Different drift limits are adopted

for the analyzed ductile (un-corroded, properly designed) and non ductile (corroded) moment resisting frame (MRF) structures (Table 3.1) as suggested in Ghobarah (2004). Thus, it has been implicitly assumed that for the $t=50$ years corrosion scenario the structures would present limited ductility compared to the initial non-corroded buildings.

Table 3.1 Damage states for Ductile and nonductile MRFs used in this study (after Ghobarah, 2004)

State of damage	Ductile MRF	Nonductile MRF
Slight/Light damage	0.4	0.2
Moderate damage	1.0	0.5
Extensive damage	1.8	0.8
Complete	3.0	1.0

3.2. Fragility functions

Fragility curves provide the conditional probability of reaching or exceeding predefined damage states as a function of a seismic intensity parameter. The overall time dependent fragility function of the buildings can be mathematically expressed as a two-parameter time-variant lognormal distribution:

$$P[DS / IM] = \Phi \left(\frac{\ln(IM) - \ln(\overline{IM}(t))}{\beta(t)} \right) \quad (3.1)$$

where, Φ is the standard normal cumulative distribution function, IM is the intensity measure of the earthquake expressed in terms of PGA (in units of g) at the ground surface, $\overline{IM}(t)$ and $\beta(t)$ are the median values (in units of g) and logarithmic standard deviations of the building fragilities at different points in time along its service life and DS is the damage state. Median values of PGA to each damage state for the different building configurations and time scenarios ($t=0$ and 50 years) were assigned based on the corresponding analytical relationships between the damage index ($ISD_{max}\%$ - dependent variable) and PGA (independent variable). Figures 3.1(a-d) present representative PGA - $ISD_{max}\%$ relationships for the low rise structures considering fixed and compliant (SSI effect for $V_{so,ave}=300\text{m/s}$) foundation conditions for the initial ($t=0$ years) and corroded ($t=50$ years) scenario. Lognormal standard deviation values $\beta(t)$ describe the total dispersion associated with each fragility curve. Three primary sources of uncertainty contribute to the total variability for any given damage state (NIBS, 2004), namely the variability associated with the definition of the limit state value, the capacity of each structural type and the seismic demand. The uncertainty in the definition of limit states is assumed to be equal to 0.4 while the variability of the capacity is assumed to be 0.25 (NIBS, 2004). The third source of uncertainty associated with the demand, is taken into consideration by calculating the variability in the results of the numerical simulations carried out in Seismostruct. Assuming that these three component dispersions are statistically independent, the total variability is expressed as the root of the sum of the squares of the component dispersions. Table 3.2 presents the median and beta values of each limit state for all the building typologies and time scenarios examined. Figure 3.2 illustrates the derived sets of fragility curves for the different building configurations for the initial non-degraded state, compared to the corresponding curves when considering corroded structural members. It is seen that the fragility curves for the corroded structures display a great shift to lower acceleration values for the same earthquake scenario. This is more pronounced for the stiffer, fixed base structures compared to the more ductile, compliant structures. Overall, similar trends are expected to occur for the low- and mid-rise structural configurations. The large differences observed generally between the curves for un-corroded and corroded frame buildings, may be partially attributed to the different damage state thresholds adopted (see Table 3.1). However, even if the same threshold is adopted, it has been shown (yet not presented herein due to space limitations) that an important increase of building vulnerability due to reinforcement corrosion is expected to take place. Moreover, as shown in the figure, the consideration of soil-foundation compliance and SSI effects may increase significantly the structure's fragility compared to the fixed base case. In particular, it is

observed that the more deformable are the soil and the foundation, the more vulnerable the structure is. This trend, however, should not be generalized as the consideration of SSI and site effects may either increase or decrease the expected structural damage depending on the type of the structure and its fundamental period in relation to the dynamic input motion and the soil properties. The modification of the soil properties during shaking is affecting the foundation compliance, and hence the two phenomena cannot be identified separately.

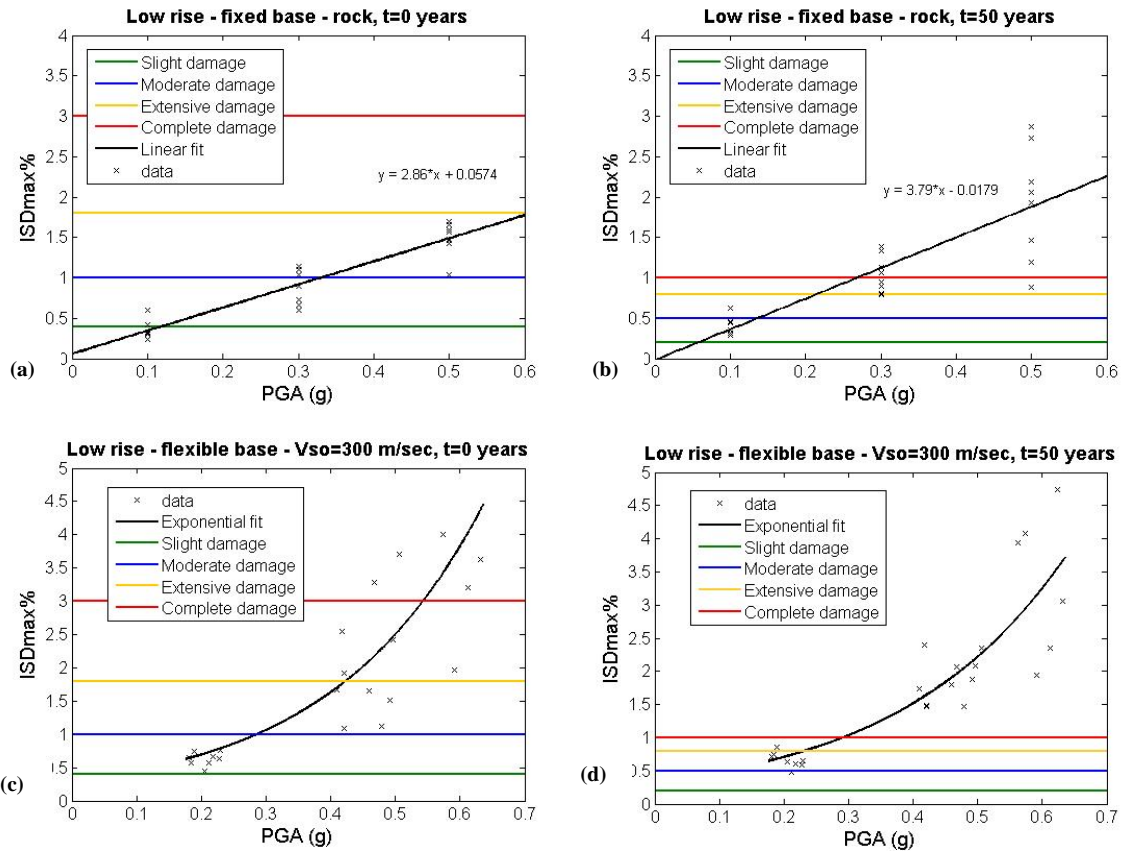


Figure 3.1. Computed PGA - ISDmax% relationships for the low rise structures considering fixed and compliant foundation conditions for the initial and corroded scenario

Table 3.2 Parameters of fragility functions

RC building	Foundation conditions	Time scenario (years)	Median PGA (g)				Dispersion
			Slight	Moderate	Extensive	Complete	
Low-rise	Fixed base -rock	t=0	0.12	0.33	0.61	1.03	0.527
		t=50	0.05	0.135	0.22	0.28	0.555
	Flexible base V _{so} =300 m/s	t=0	0.15	0.28	0.43	0.62	0.529
		t=50	0.1	0.18	0.25	0.29	0.578
	Flexible base V _{so} =200 m/s	t=0	0.05	0.14	0.27	0.49	0.530
		t=50	0.04	0.08	0.12	0.15	0.640
Mid-rise	Fixed base -rock	t=0	0.13	0.35	0.63	1.06	0.568
		t=50	0.06	0.129	0.23	0.29	0.720
	Flexible base V _{so} =300 m/s	t=0	0.17	0.38	0.51	0.62	0.600
		t=50	0.12	0.21	0.29	0.34	0.676
	Flexible base V _{so} =200 m/s	t=0	0.08	0.17	0.27	0.41	0.646
		t=50	0.06	0.11	0.17	0.20	0.688

4. CONCLUSIONS

The seismic vulnerability of RC frame buildings has been assessed taking into account foundation

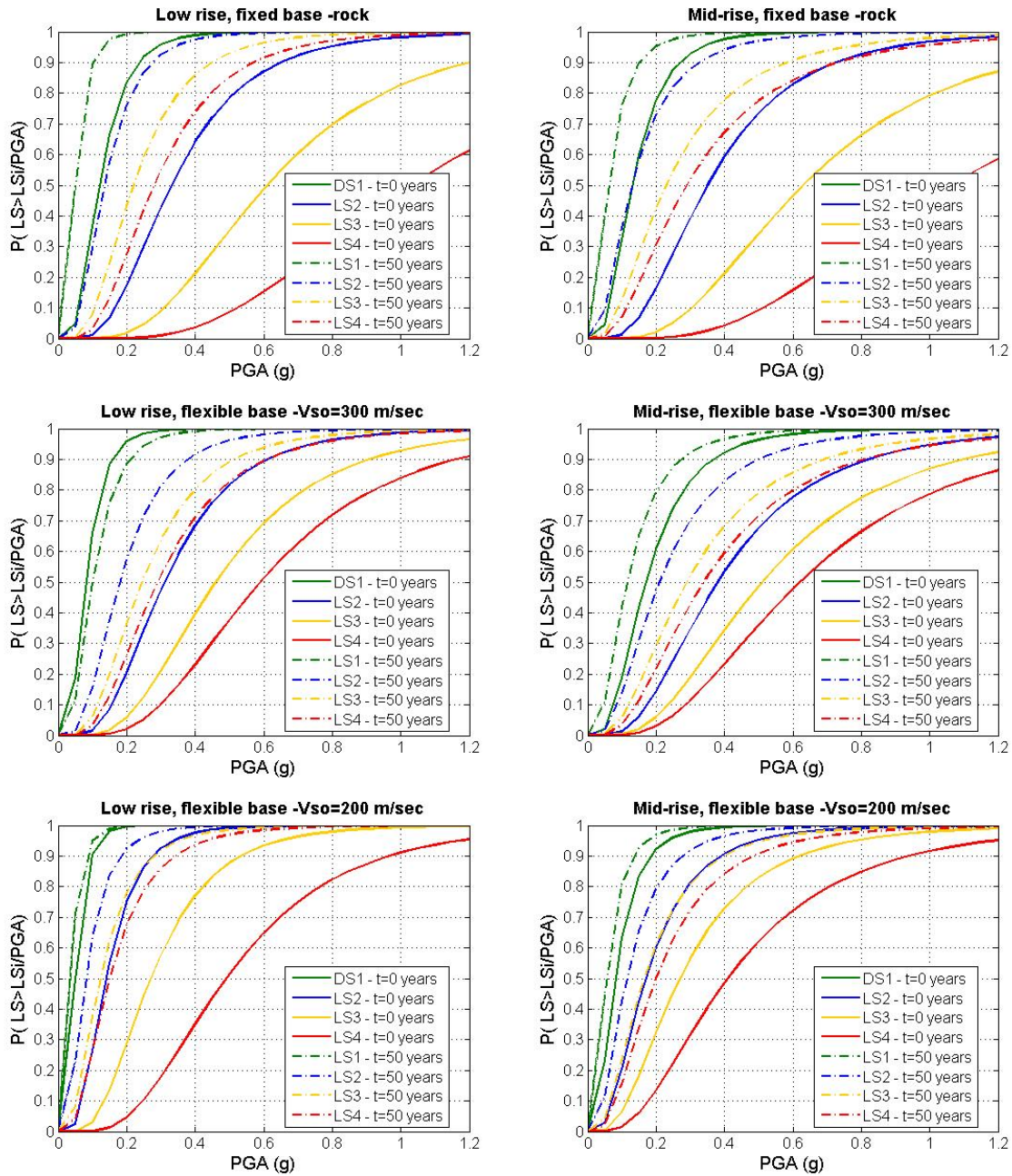


Figure 3.2. Fragility curves for the low rise (left) and mid-rise structures (right) considering fixed and compliant ($V_{so}=200, 300$ m/sec) foundation conditions for the initial ($t=0$ years) and corroded ($t=50$ years) scenario

compliance, SSI effects and the corrosion of the RC structural members. Both low and mid-rise bare frame structures were analyzed using 2D nonlinear dynamic computations. Time-dependent probabilistic fragility functions have been derived for predefined selected damage states for two time periods ($t=0, 50$ years) in terms of peak ground acceleration at the base of the structure for all the building typologies considered. It has been showed that the reinforcement corrosion may result to a significant increase of the structures' fragility. The consideration of soil deformability and foundation compliance has been found to modify the structural response of the analyzed structures resulting to higher vulnerability values. However, this should not be regarded as a general trend as the seismic structural vulnerability may decrease or increase depending on the characteristics of the building, the input motion and the soil properties. Moreover in order to increase the robustness of the preliminary conclusions presented herein, further research is needed in the definition of limit states for corroded structures based on adequate analytical, experimental and empirical data and the incorporation of the

fully probabilistic corrosion models within the dynamic analysis. In summary the results presented prove that eventually the fragility curves used so far for RC buildings under fixed base conditions and assuming no aging effects, may, under certain circumstances, underestimate the real vulnerability of the structures.

ACKNOWLEDGEMENT

Most of the work reported in this paper was carried out in the framework of the ongoing REAKT (<http://www.reaktproject.eu/>) project, funded by the European Commission.

REFERENCES

- Abo El Ezz, A. (2008). Deformation and strength based assessment of seismic failure mechanisms for existing RC frame buildings, Master dissertation, Rose School, Pavia.
- BRGM (French Geological Survey) Software (1998) Cyberquake, version 1.1. User's guide.
- CEB-FIB Task Group 5.6 (2006), Model Code for Service Life Design. Bulletin 31, fédération internationale du béton (fib), 2006.
- Choe, D.-E., Gardoni, P. and Rosowsky, D. (2010). Fragility Increment Functions for Deteriorating Reinforced Concrete Bridge Columns, *Journal of Engineering Mechanics* **136:8**, 969- 978.
- Choe, D.-E., Gardoni, P., Rosowsky, D. And Haukaas, T., (2009). Seismic fragility estimates for reinforced concrete bridges subject to corrosion, *Structural Safety* **31**, 275–283.
- Darendeli, M. (2001). Development of a new family of normalized modulus reduction and material damping curves, Ph.D. Dissertation, Univ. of Texas.
- DuraCrete (1998). Modeling of Degradation. BRITE –EURAM-Project BE95-1347/R4-5.
- DuraCrete (2000). Probabilistic Performance Based Durability Design of Concrete Structures: Statistical Quantification of the Variables in the Limit State Functions. Report No.: BE 95-1347, pp. 62-63.
- EAK2000 (2000). Greek Seismic Code, Organization of Seismic Planning and Protection.
- Gelagoti, F. (2010). Metaplastic Response and Collapse of Frame–Foundation Systems, and the Concept of Rocking Isolation, Ph.D. Dissertation, National Technical University of Athens.
- Ghobarah, A. (2004). On Drift Limits Associated with Different Damage Levels, *International Workshop on Performance-Based Seismic Design*, Department of Civil Engineering, McMaster University, Ontario, Canada, June 28 - July 1.
- Ghosh, J. and Padgett, J.E., (2010). Aging Considerations in the Development of Time-Dependent Seismic Fragility Curves, *Journal of Structural Engineering* **136: 12**, 1497-1511.
- Kwok, A. O. L., Stewart, J. P., Hashash, Y. M., Matasovic, N., Pyke, R., Wang, Z. and Yang, Z. (2007). Use of Exact Solutions of Wave Propagation Problems to Guide Implementation of Nonlinear Seismic Ground Response Analysis Procedures, *Journal of Geotechnical and Geoenvironmental Engineering* **133:11**, 1385-1398.
- Mander, J. B., Priestley, M. J. N., and Park, R. (1988). Theoretical stress-strain model for confined concrete, *Journal of Structural Engineering* **114:8**, 1804-1826.
- Mylonakis, G., Nikolaou, S. and Gazetas, G. (2006). Footings under seismic loading: Analysis and design issues with emphasis on bridge foundations, *Soil Dynamics and Earthquake Engineering* **26**, 824–853.
- National Institute of Building Sciences (2004). Direct Physical Damage - General Building Stock. HAZUS-MH Technical manual, Chapter 5, Federal Emergency Management Agency, Washington, D.C.
- Priestley, M.J.N. and Grant, D.N. (2005). Viscous damping in seismic design and analysis, *Journal of Earthquake Engineering* **9:1**, 229-255.
- SeismoSoft (2011). SeismoStruct – A computer program for static and dynamic nonlinear analysis of framed structures, (online): Available from URL: www.seismosoft.com
- Stewart, M. (2004). Spatial variability of pitting corrosion and its influence on structural fragility and reliability of RC beams in flexure, *Structural Safety* **26**, 453–470.
- Sæz, E., Lopez-Caballero, F. and Modaressi-Farahmand-Razavi, A. (2011). Effect of the inelastic dynamic soil–structure interaction on the seismic vulnerability assessment. *Structural Safety* **33**, 51-63.
- Yalciner, H., Sensoy, S. and Eren, O.(2012). Time-dependent seismic performance assessment of a single-degree-of-freedom frame subject to corrosion, *Engineering Failure Analysis* **19**, 109–122.